Wideband tunable wavelength-selective coupling in asymmetric side-polished fiber coupler with dispersive interlayer

Nan-Kuang Chen[1,*], Cheng-Ling Lee[1], and Sien Chi[2,3]

[1]*Department of Electro-Optical Engineering, National United University, Miaoli, Taiwan 360, R.O.C.*
[2]*Department of Photonics, National Chiao Tung University, Hsinchu, Taiwan 300, R.O.C.*
[3]*Department of Electrical Engineering, Yuan Ze University, Chungli, Taiwan 320, R.O.C.*
**Corresponding author: nkchen@nuu.edu.tw*

Abstract: We demonstrate tunable highly wavelength-selective filter based on a 2×2 asymmetric side-polished fiber coupler with dispersive interlayer in one of the coupling arms. The asymmetric fiber coupler is made of two side-polished fibers using identical single-mode fibers and one of the polished fibers is further chemically etched at the central evanescent coupling region to gain closer to the core. An optical liquid with different dispersion characteristics than that of silica fiber is used to fill up the etched hollow and therefore the propagation constant for the polished fiber with dispersive liquid becomes more dispersive and crosses with that of another untreated polished fiber. The location of the cross point and the cross angle between two propagation constant curves determine the coupling wavelength and coupling bandwidth as well as channel wavelength separation, respectively. The coupling wavelength can be tuned at least wider than 84 nm (1.326-1.410 μm) under index variation of 0.004 and with coupling ratios of higher than 30 dB.

OCIS codes: (060.1810) Buffers, couplers, routers, switches, and multiplexers; (060.2340) Fiber optics components; (260.2030) Dispersion; (160.6840) Thermo-optical materials.

References and links

1. M. Sumetsky, Y. Dulashko, and M. Fishteyn, "Demonstration of a multi-turn microfiber coil resonator," in Proc. of OFC 2007, PDP46 (2007).
2. C. Vazquez, S. E. Vargas, and J. M. S. Pena, "Sagnac loop in ring resonators for tunable optical filters," J. Lightwave Technol. **23**, 2555-2567 (2005).
3. E. Wikszak, J. Thomas, J. Burghoff, B. Ortaç, J. Limpert, S. Nolte, U. Fuchs, and A. Tünnermann, "Erbium fiber laser based on intracore femtosecond-written fiber Bragg grating," Opt. Lett. **31**, 2390-2392 (2006).
4. G. P. Agrawal, *Fiber-Optic Communication Systems*, (Wiley-Interscience, New York, 1997), Chap. 7.
5. A. K. Das and M. A. Mondal, "Precise control of the center wavelength and bandwidth of wavelength-selective single-mode fiber couplers," Opt. Lett. **19**, 795-797 (1994).
6. N. K. Chen, S. Chi, and S. M. Tseng, "Wideband tunable fiber short-pass filter based on side-polished fiber with dispersive polymer overlay," Opt. Lett. **29**, 2219-2221 (2004).
7. N. J. C. Libatique, L. Wang, R. K. Jain, "Single-longitudinal-mode tunable WDM-channel-selectable fiber laser," Opt. Express **10**, 1503-1507 (2002).
8. A. W. Snyder and Y. Chen, "Nonlinear fiber couplers: switches and polarization beam splitters," Opt. Lett. **14**, 517-519 (1989).
9. C. W. Wu, T. L. Wu, and H. C. Chang, "A novel fabrication method for all-fiber, weakly fused, polarization beamsplitters," IEEE Photon. Technol. Lett. **7**, 786-788 (1995).
10. K. Morishita, "Wavelength-selective optical-fiber directional couplers using dispersive materials," Opt. Lett. **13**, 158-160 (1988).
11. R. Zengerle and O. Leminger, "Narrow-band wavelength-selective directional couplers made of dissimilar single-mode fibers," J. Lightwave Technol. **LT-5**, 1196-1198 (1987).

#88294 - $15.00 USD Received 5 Oct 2007; revised 7 Dec 2007; accepted 10 Dec 2007; published 12 Dec 2007

12. C. J. Chung and A.Safaai-Jazi, "Narrow-band spectral filter made of W-index and step-index fibers," J. Lightwave Technol. **10**, 42-45 (1992).
13. O. Leminger and R. Zengerle, "Narrow-band directional couplers made of dissimilar single-mode fibers with different cladding refractive indexes," J. Lightwave Technol. **8**, 1289-1291 (1990).
14. B. Malo, F. Bilodeau, K. O. Hill, D. C. Johnson, and J. Albert, "Unbalanced dissimilar-fibre Mach-Zehnder interferometer: application a filter," Electron. Lett. **25**, 1416-1417 (1989).
15. X. Su, A. Tan, X. Jia, Q. Pan, C. Xie, and K. Peng, "Experimental demonstration of quantum entanglement between frequency-nondegenerate optical twin beams," Opt. Lett. **31**, 1133-1135 (2006).
16. N. K. Chen, S. Chi, and S. M. Tseng, "Narrow-band channel-dropping filter based on side-polished fiber with long interaction length," Jpn. J. Appl. Phys. **43**, L475-L477 (2004).
17. O. Parriaux, S. Gidon, and A. A. Kuznetsov, "Distributed coupling on polished single-mode optical fibers," Appl. Opt. **20**, 2420-2423 (1981).
18. M. J. F. Digonnet and H. J. Shaw, "Analysis of a tunable single mode optical fiber coupler," IEEE J. Quan. Electron. **QE-18**, 746-754 (1982).
19. M. J. F. Digonnet, J. R. Feth, L. F. Stokes, and H. J. Shaw, "Measurement of the core proximity in polished fiber substrates and couplers," Opt. Lett. **10**, 463-465 (1985).
20. M. J. F. Digonnet, "Passive and Active Fiber Optic Components," Ph. D. Dissertation, Stanford University (1983).
21. T. Erdogan, "Fiber grating spectra," J. Lightwave Technol. **15**, 1277-1294 (1997).

1. Introduction

Variant kinds of fiber filters are essential to filter out the desired wavelengths from the optical fibers for signal routing and processing. The fiber filters with a simple architecture, high extinction ratio, moderate filtering bandwidth, wide tuning range, and high tuning efficiency can greatly favor the fiber-optic communication and sensing systems. In general, the fiber filters can be made in interferometric forms, e.g., micro-coil, Sagnac, Mach-Zehnder, Fabry-Perot, and Bragg grating [1-4], or in non-interferometric forms, e.g., stimulated Brillouin scattering, coupler, short-pass, and absorption [4-7]. Among them, non-interferometric filters such as coupler filters may usually have wider filtering bandwidth, wider tuning range, superior environment stability, and be more cost-effective than the interferometric filters. The fiber coupler can serve as not only power splitter and wavelength multiplexer but also spectral filters, switches, and polarization beamsplitters [8, 9]. For symmetric couplers, some specific wavelengths satisfying the phase matching condition can be filtered out from the input bus and then come out from the cross-coupling port with a typical spectral response of quasi-periodic oscillation. However, only one wavelength that can satisfy the phase matching condition and to be filtered out over a wide spectral range is sometimes necessary. Asymmetric fiber couplers using dissimilar fibers had been proposed to achieve the spectral filters with only one coupling wavelength over a few hundreds of nanometers based on material dispersion [10] or waveguide dispersion [11-13] discrepancy between two fibers. When the difference between two mode field distributions (MFDs) of the coupling fibers is large enough, the propagation constants of the two fibers turn out to have very different wavelength-dependent behaviours [10-13]. Accordingly, the phase matching for optical coupling between two fibers can only be satisfied at a specific wavelength, namely, the cross point of propagation constant curves (PCCs). The location of the cross point determines the coupling wavelength while the cross angle between the two PCCs controls the coupling bandwidth. These coupler filters are simple, environment stable and could also realize highly unbalanced Mach-Zehnder interferometers [14, 15]. Nevertheless, the coupling wavelength is not tunable and, at least, one special fiber is required for these asymmetric couplers.

In this paper, we, for the first time, demonstrate thermooptic-tunable coupler filters based on an asymmetric side-polished fiber (SPF) coupler using two identical standard single-mode fibers. In the beginning, the propagation constants of two SPFs are in a similar wavelength-dependent behaviour and the coupler has oscillating power transfer cycles. After a dispersive material is locally introduced in one of the coupling arms shown in Fig 1, power coupling becomes highly wavelength-selective. In Fig. 1, one normal SPF is further processed by

#88294 - $15.00 USD Received 5 Oct 2007; revised 7 Dec 2007; accepted 10 Dec 2007; published 12 Dec 2007

locally etching the central evanescent coupling region using hydrofluoric acid to generate a hollow, which contains the optical liquid with quite different dispersion characteristics than that of SPFs, so that the MFDs of the guiding lights are substantially altered. Accordingly, the composite dispersion characteristic of the etched SPF turns out to be significantly different from that of the original SPF and thus the two PCCs of this coupler will cross at a point where coupling occurs. The coupling ratios of our coupler filters can be higher than 30 dB and are qualified as high isolation demultiplexers. The wavelength tunability is as wide as 84 nm (1.326-1.410 μm) under index variation of 0.004 and the tuning efficiency is estimated to be higher than 8 nm/°C.

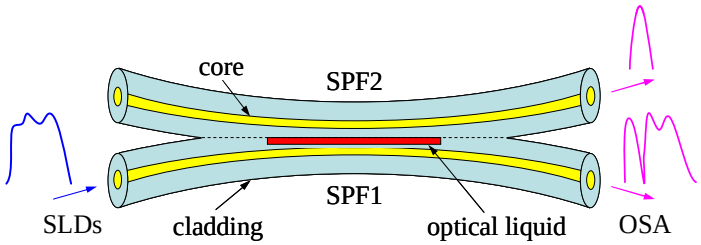

Fig. 1. Device structure of the coupler filter where an optical liquid is introduced in one of the coupling arms.

2. Device structure and fabrication

In fabrication of SPF, a section jacket of the single-mode fibers (Corning: SMF-28) was striped off and the bare section was then embedded and glued into a curved Si V-groove with radius of curvature of 15 m which leads to an effective interaction length L_{eff} of around 11 mm [16]. The exposed cladding was polished away until the strong evanescent field was accessible and the remained central cladding thickness was around 0.5 μm. The particle size of the polishing slurry was about 50 nm to reduce surface roughness of SPF for avoiding scattering loss. For the purpose of rapid and precision alignment in transverse direction, two straight V-grooves with a little bit smaller size than that for SPF were prepared alongside the SPF on Si wafer for each piece of sample. When these two straight V-grooves of first sample were vertically mated with another two straight V-grooves of second sample up and down to achieve two new rhombus grooves, a dummy optical fiber with suitable diameter can be embedded in each rhombus groove to automatically align the SPFs (SPF1 and SPF2) as a fiber coupler in the transverse direction [16]. A white-light source spanning 1.25-1.65 μm comprising multiple superluminescent diodes (SLDs) was launched into input port of the fiber coupler to investigate the coupling characteristics by optical spectrum analyzer (OSA) (Advantest: Q8381). The spectral responses of power coupling showed quasi-periodic oscillations and the maximum transferred power was about 70% with the channel wavelength separation of 42 nm at 1.55 μm band. Subsequently, the mated SPFs were separated and a drop of hydrofluoric acid was applied on the central evanescent coupling region of SPF1 to locally etch part of the remained cladding away. The etched length and depth were estimated 7.6 mm under microscope and 0.3 μm by etching-rate, respectively. Finally, the SPF1 and SPF2 were again recombined as a fiber coupler while a low-index Cargille liquid, which has a much lower dispersion than that of silica fiber [6], was used to fill up the etched hollow in SPF1 and the mated SPFs were longitudinally tuned by a precision micrometer with respect to each other to find out an optimized coupling. A thermoelectric cooler may be used beneath the silicon wafer to control the heating temperature for the optical liquid so that the refractive index dispersion n(λ) curve of optical liquid will change and will thus move the cross point of PCCs of the coupler in future works.

#88294 - $15.00 USD Received 5 Oct 2007; revised 7 Dec 2007; accepted 10 Dec 2007; published 12 Dec 2007

3. Numerical and experimental analysis

For conventional side-polished fiber couplers [17-20], index matching liquid was usually employed in between the SPFs to fill up the air gap and enhance optical coupling. However, the fiber coupler with only one coupling wavelength over a wide spectral range had never been achieved when the coupler was made of identical fibers. A substantial asymmetry of the MFDs at two coupler halves was not realized even though an optical liquid with quite different dispersion than silica fiber was used in between mated SPFs. Intuitively, the dispersion characteristics of one of the coupler halves can be significantly changed if the optical liquid physically belongs to this coupler half only. In order to achieve that, the MFD of the guiding lights must heavily overlap the optical liquid and thus a discontinuity of the cladding at evanescent field region is required to enforce the lights passing through the optical liquid. If the optical liquid is applied on the standard SPF, whose remained cladding thickness gradually increases toward bilateral ends like an adiabatic situation, the MFD will still mainly pile up around the core and the dispersion is not substantially altered. In contrast, the etched hollow can introduce a discontinuity of cladding at evanescent field region and thus the MFD strongly overlap the optical liquid filling up the hollow to cause dispersion mismatch between the coupler halves. The resulting PPCs cross each other at a point and thus only one coupling wavelength can satisfy the phase matching condition and to be cross-coupled into the output port at the other side.

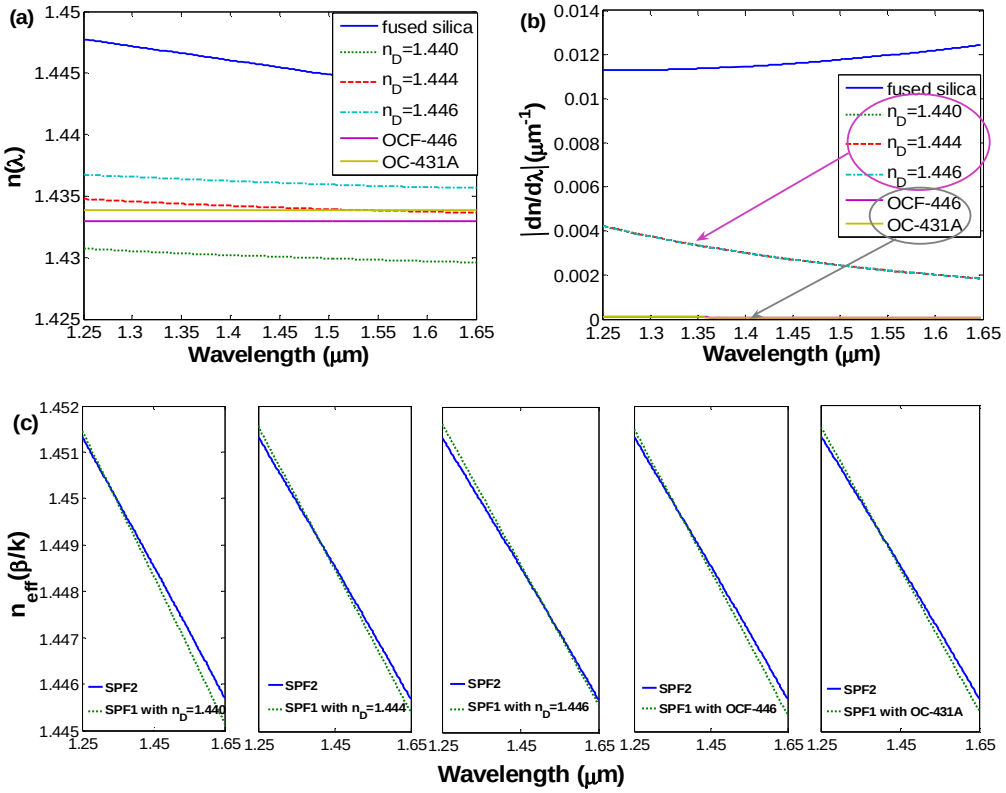

Fig. 2. (a) Refractive index dispersion curves of silica, Cargille liquids (n_D = 1.440, 1.444, 1.446), and optical polymers (OCF-446, OC-431A). (b) Dispersion slope of the silica, Cargille liquids (n_D = 1.440, 1.444, 1.446), and optical polymers (OCF-446, OC-431A). (c) Effective indices of the SPF1 with optical materials and SPF2.

#88294 - $15.00 USD Received 5 Oct 2007; revised 7 Dec 2007; accepted 10 Dec 2007; published 12 Dec 2007

In numerical simulation, the radii of curvature for the coupler halves are both of 15 m and the coupling coefficient for a specific wavelength varies from position to position and is different when light is respectively incident from SPF1 and SPF2. In this work, the input port is at the side of SPF1 and the PCC of SPF1, $\beta_1(\lambda)$, is actually the composite of the optical material and the fused silica with a weighting ratio. The thickness of optical material and remained cladding at central evanescent coupling region is 0.3 μm and 0.2 μm, respectively. The refractive index dispersion of silica, optical liquids (Cargille: n_D = 1.440, 1.444, 1.446), and optical polymers (Nye Lubricants: OCF-446, OC-431A) are shown in Fig. 2(a) while their dispersion slopes are shown in Fig. 2(b). By solving the characteristic equation of fiber, the effective indices n_{eff} for SPF1 comprising variant optical materials and SPF2 are shown in Fig. 2(c). Apparently, the SPF1 with a less dispersive optical material will result in a more dispersive n_{eff} because the MFDs of the shorter wavelengths are more strongly confined and the $\beta_1(\lambda)$ can thus cross the PCC of SPF2, $\beta_2(\lambda)$. The cross point means that the phase matching condition can only occur at this wavelength over the whole spectral range. The cross angle between the PCCs controls the coupling bandwidth and a less dispersive optical liquid e.g., n_D = 1.440 is expected to produce a narrowest coupling bandwidth. By coupled-mode theory, the spectral responses of using variant optical materials at the direct-through and cross-coupling ports for this asymmetric coupler with dispersive interlay are simulated and shown in Fig. 3(a). The spectra were simulated with the optimized coupling length shorter than the L_{eff} for each optical material and thus overcoupling may be chosen for desired coupling bandwidth. In Fig. 3(a), the optimized coupling lengths for the spectra from top to down in simulations are 6.87 mm, 6.19 mm, 7.80 mm, 7.13 mm, 6.37 mm, respectively. The distance, from center to center, between the two cores at central evanescent coupling region is 9.2 μm and the radius of core is 4.1 μm. Based on coupled-mode theory, the coupling bandwidth is proportional to the coupling length, coupling coefficient, and the effective index difference Δn_{eff} between SPF1 and SPF2 [21]. A longer coupling length is especially effective to obtain a narrower coupling bandwidth [21]. However, the SPFs constituting the asymmetric coupler are transversely locked by dummy fibers to accomplish a rapid alignment, which can be usually down in 1-2 minutes, the coupling coefficient and coupling length can not be largely changed to achieve optimal coupling for the coupling wavelengths over wide spectral range like in Digonnet's experiments [20] while longitudinally tuning the relative position of SPFs. From Fig. 3(a)-1, the simulated spectra show that this asymmetric coupler can also play as high-isolation (de)multiplexers. The channel isolation between 1.326 μm and 1.444 μm wavelength can be both higher than 30 dB and the channel spacing is 118 nm. The channel spacing can be further tunable by using optical materials with different dispersion slopes and tuning to a suitable temperature to move to fit the specific coupling wavelength.

In measurements, Figs. 3(b) show the transmission spectra from direct-through port of the coupler filter using different index liquids. When the refractive indices of the Cargille liquids in etched hollow at 25°C were 1.444 (n_D) and 1.440 (n_D), the corresponding spectral responses are shown in Fig. 3(b)-2 and 3(b)-3, respectively. Fig. 3(b)-1 is the original SLDs transmission spectrum passing through etched SPF before mating as a coupler. In Fig. 3(b)-2 and 3(b)-3, the coupling wavelengths occur at 1.410 μm and 1.326 μm, respectively, due to the cross of $\beta_1(\lambda)$ and $\beta_2(\lambda)$, and both of their coupling ratios are above 30 dB. The coupling wavelength moves from 1.410 μm to 1.326 μm when the indices of liquids are changed from 1.444 to 1.440 and the corresponding coupling length was varied by longitudinally fine tuning the relative position of SPFs using a micrometer to satisfy the phase matching condition for the new coupling wavelength. This index variation of 0.004 is corresponding to temperature variation of +10.5°C because the thermo-optic coefficients of the index liquids are both about -3.82×10^{-4}/°C. From Fig. 3(b)-2 and 3(b)-3, the coupling wavelength moves toward the shorter wavelength when the index of the Cargille liquid decreases. This is because a lower index of Cargille liquid can make the effective index of $\beta_1(\lambda)$ reduced, compared to that of $\beta_2(\lambda)$, and thus the cross point between two PCCs move toward the shorter wavelengths, see Fig. 2(c). On the other hand, when the index of Cargille liquid decreases from 1.444 to 1.440,

#88294 - $15.00 USD Received 5 Oct 2007; revised 7 Dec 2007; accepted 10 Dec 2007; published 12 Dec 2007

the resulting coupling bandwidth turns into much narrower due to a larger Δn_{eff}. From Figs. 3(b)-1 and 3(b)-2, the insertion loss for the passband at direct-through port at 1314 nm and 1548 nm is about 1 dB and 1.5 dB, respectively. However, from Figs. 3(b)-1 and 3(b)-3, the insertion loss for the passband at direct-through port at 1630 nm is about 3.5 dB where the Figs. 3(b)-1 and 3(b)-3 are in different resolution (RES) of OSA and power division (D) scale. The higher insertion losses in Fig. 3(b)-3 are due to the larger index difference Δn between the optical liquid and the silica cladding. A larger Δn can excite higher order modes for the guiding lights in the transverse direction of the liquid-filled etched hollow region to suffer more optical losses. This will be improved by dry etching the remained silica cladding right above the core so that the excitations of higher order modes can be suppressed.

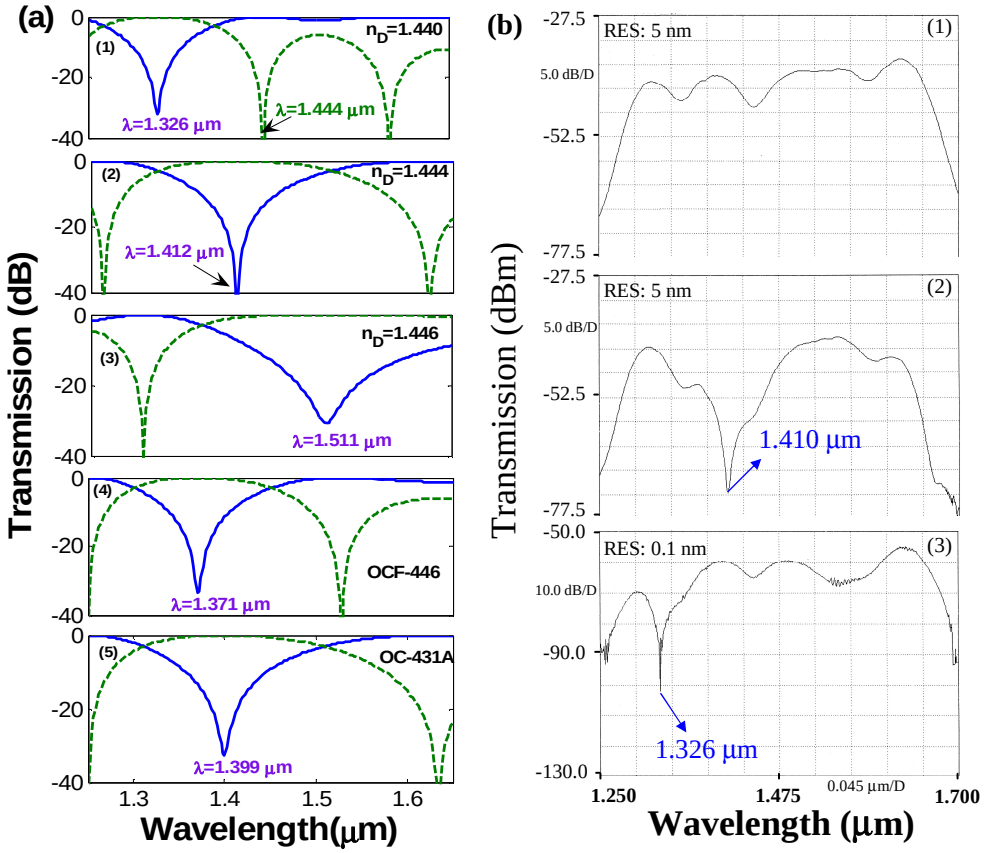

Fig. 3. (a) Simulated spectral responses of the asymmetric coupler with variant dispersive interlayers and (b) experimental results of the transmission spectra using optical liquids under different optical resolution of OSA.

4. Conclusion

In conclusion, we have demonstrated and analyzed the tunable highly wavelength-selective couplers with a coupling ratio of higher than 30 dB based on an asymmetric side-polished fiber coupler using identical single-mode fibers. The tuning range of the coupling wavelength can at least covers 1.326-1.410 μm with an estimated tuning efficiency of 8 nm/°C. The coupling wavelength and coupling bandwidth is respectively controllable by the index and dispersion slope of the filled dispersive materials. The channel wavelength separation and coupling bandwidth are both tunable and wider than a few tens of nanometers, which could be

#88294 - $15.00 USD Received 5 Oct 2007; revised 7 Dec 2007; accepted 10 Dec 2007; published 12 Dec 2007

useful for as wavelength-selective filters in supercontinuum light-source or in broadband amplifiers. This component could also serve as tunable high-isolation (de)multiplexers, band-pass/stop filters and key elements in highly unbalanced tunable Mach-Zehnder interferometers.

Acknowledgments

This work was funded by grants from the Republic of China National Science Council (NSC 96-2221-E-155-039-MY3, NSC 96-2221-E-239-014, NSC 96-2752-E-009-009-PAE) and the National Chiao Tung University (MOE ATU Program).

#88294 - $15.00 USD Received 5 Oct 2007; revised 7 Dec 2007; accepted 10 Dec 2007; published 12 Dec 2007